Journal of Cellular Biochemistry 98:1296–1307 (2006)

Loss of Phosphatase Activity in *Ptp69D* Alleles Supporting Axon Guidance Defects

Joy E. Marlo[1]* and Chand J. Desai[1,2]

[1]Department of Pharmacology, Vanderbilt University Medical Center, Nashville, Tennessee 37232
[2]Vanderbilt Center for Molecular Neuroscience, Vanderbilt University Medical Center, Nashville, Tennessee 37232

Abstract PTP69D is a receptor protein tyrosine phosphatase that was identified as a key regulator of neuromuscular axon guidance in *Drosophila*, and has subsequently been shown to play a similar role in the central nervous system and retina. Three *Ptp69D* alleles with mutations involving catalytically important residues exhibit a high degree of phenotypic variation with viability of mutant adult flies ranging from 0 to 96%, and ISNb motor nerve defects ranging from 11 to 57% [Desai and Purdy, 2003]. To determine whether mutations in *Ptp69D* affecting axon guidance and viability demonstrate losses of phosphatase activity and whether differences in catalytic potential underlie phenotypic variability, we expressed full-length wild-type and mutant PTP69D protein in Schneider 2 cells, and assessed phosphatase activity using the fluorogenic substrate 6,8-difluoro-4-methylumbelliferone phosphate (DiFMUP). Detailed biochemical characterization of wild-type PTP69D, including an examination of sensitivity to various inhibitors, in vitro catalytic efficiency, and the pH-k_{cat} profile of the enzyme, suggests a common tyrosine phosphatase reaction mechanism despite lack of sequence conservation in the WPD loop. Analysis of mutant proteins revealed that every mutant had less than 1% activity relative to the wild-type enzyme, and these rates did not differ significantly from one another. These results indicate that mutations in *Ptp69D* resulting in axon guidance defects and lethality significantly compromise catalytic activity, yet the range of biological activity exhibited by *Ptp69D* mutants cannot be explained by differences in catalytic activity, as gauged by their ability to hydrolyze the substrate DiFMUP. J. Cell. Biochem. 98: 1296–1307, 2006.

Key words: PTP; catalytic; DiFMUP; kinetics; axon guidance

Conserved from invertebrates to mammals, receptor protein tyrosine phosphatases (RPTPs) are expressed on the growth cones and axons of outgrowing neurons where they are poised to couple extracellular guidance cues to intracellular effectors that mediate cytoskeletal rearrangement [Desai et al., 1997b; Stoker, 2001; Johnson and Van Vactor, 2003; Ensslen-Craig and Brady-Kalnay, 2004]. Genetic studies in *Drosophila* have indicated broad functions for PTP69D, a type IIa receptor phosphatase, in guiding axon trajectories in the central and peripheral nervous system and in the retina. Mutations in this essential gene cause embryonic and larval lethality, partially penetrant defects in guidance of ISNb motor nerve axons, and highly penetrant defects in the guidance of R1-R6 photoreceptor axons [Desai et al., 1996, 1997a; Garrity et al., 1999; Newsome et al., 2000; Sun et al., 2000a, 2001].

Consistent with functions in signaling, a large extracellular domain (ECD) and tandem intracellular phosphatase domains characterize most classical tyrosine-specific RPTPs (Fig. 1). Within the intracellular domain (ICD), the membrane-proximal (D1) phosphatase domain possesses

Abbreviations used: ISNb, intersegmental nerve b; DiFMUP, 6,8-difluoro-4-methylumbelliferone phosphate; ECD, extracellular domain; ICD, intracellular domain; PTP, protein tyrosine phosphatase; E-P, phosphoenzyme intermediate.

Grant sponsor: National Institutes of Health, Training Grant in Developmental Biology, Vanderbilt University; Grant number: HD07502; Grant sponsor: National Institutes of Health; Grant number: 1RO1-NSHD38141; Grant sponsor: March of Dimes; Grant number: MOD 5-FY99-0111.

*Correspondence to: Joy E. Marlo, 406 RRB, 23rd Avenue South at Pierce, Nashville, TN 37232.
E-mail: joy.marlo@vanderbilt.edu.

Received 10 December 2005; Accepted 17 January 2006
DOI 10.1002/jcb.20862

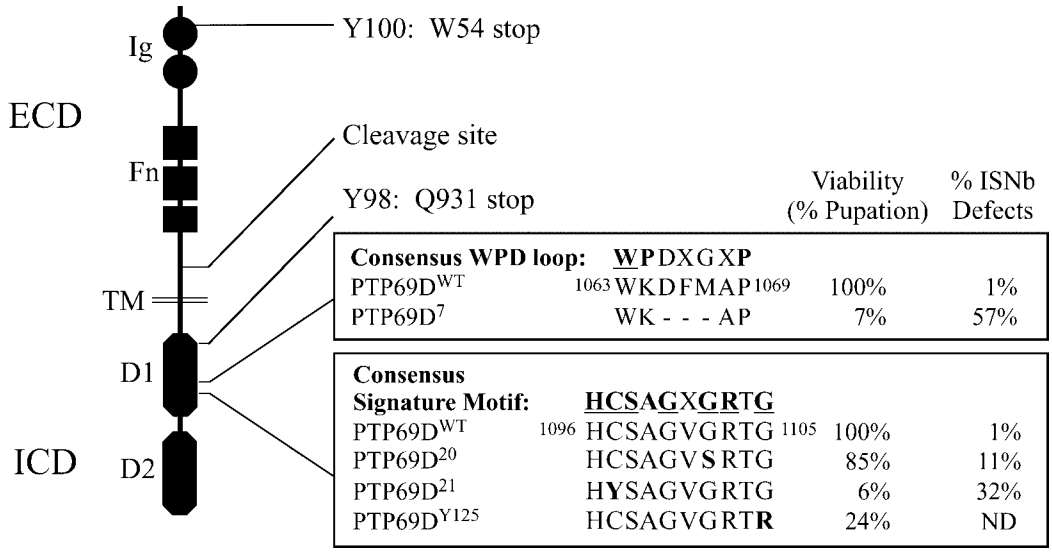

Fig. 1. Schematic of PTP69D, showing regions of the protein affected by mutations. Circles represent immunoglobulin (Ig) domains, squares represent fibronectin (Fn) type III repeats, and octagons represent tandem phosphatase domains (D1 and D2). The extracellular domain (ECD), intracellular domain (ICD), transmembrane domain (TM), and site of cleavage in the ECD are labeled for orientation. *Ptp69D*^{Y100} and *Ptp69D*^{Y98} encode early C-terminal truncation products (Y100 and Y98). Consensus sequences of the WPD loop and active site (signature motif) are shown, and wild-type PTP69D amino acids are numbered. Amino acids with 90% or greater conservation among PTPs in consensus sequences are in bold type, and underscored amino acids are invariant [Andersen et al., 2001]. Interestingly, PTP69D^{WT} differs from the PTP consensus sequence of the WPD loop. The *Ptp69D*^{7} allele has a deletion removing amino acids 1065–1067 (DFM) in the WPD loop. *Ptp69D*^{20}, *Ptp69D*^{21}, and *Ptp69D*^{Y125} all contain missense mutations in the active site, which are also in bold type. To the right of PTP69D amino acid sequences is phenotypic data from [Desai and Purdy, 2003] showing viability rates (in percent of expected pupa) and the severity of axon guidance defects using the ISNb motor nerve as a marker for PTP69D activity.

most or all of the in vitro catalytic activity of RPTP protein, while the distal (D2) domain is thought to regulate activity, substrate specificity, or localization.

Genetic structure-function studies have shown that extracellular and intracellular mutations in RPTPs can independently disrupt their functions, suggesting that signals initiated by the ECD are converted into intracellular signals by the ICD [Garrity et al., 1999; Newsome et al., 2000; Maurel-Zaffran et al., 2001; Sun et al., 2001; Desai and Purdy, 2003; Krueger et al., 2003]. Several lines of evidence have suggested that the catalytic activity of RPTPs is required for at least some of their in vivo functions. Inhibition of RPTPs by classical inhibitors, by oxidation, or by forced dimerization, abrogates certain PTP-mediated responses. For example, steering of chick forebrain growth cones mediated by PTPδ can be disrupted using the classical PTP inhibitor vanadate [Sun et al., 2000b]. Inhibition of PTP activity in B cells, by the generation of reactive oxygen species, appears to relieve tonic negative regulation of the antigenic response [Singh et al., 2005; Tonks, 2005]. Moreover, forced dimerization of PTPα decreases its ability to dephosphorylate and activate c-Src in fibroblasts [Jiang et al., 1999]. Further evidence for the role of catalytic activity in PTP signaling comes from the observation that mutations in highly conserved active-site residues are associated with strong loss of function phenotypes. In *C. elegans Clr-1*, a RPTP gene closely related to *Ptp69D*, three alleles perturbing the active site confer severe defects in body morphology. Finally, catalytically inactive forms of PTPs fail to rescue some, though not all, mutant phenotypes of *Clr-1*, *Dlar*, and *Ptp69D* in transgene rescue experiments [Kokel et al., 1998; Garrity et al., 1999; Newsome et al., 2000; Sun et al., 2001; Krueger et al., 2003].

Interestingly, some PTP-mediated effects may be activity-independent; for example, although many of the functions of CD45 require its phosphatase activity, crosslinking of either wild-type or inactive CD45 with monoclonal antibodies triggers apoptotic cell death in T cells [Fortin et al., 2002]. Similarly, transgene rescue experiments have suggested that the catalytic

activity of PTP69D may not be required for all of its in vivo functions in *Drosophila*. The D2 domain alone, which in most RPTPs is catalytically inactive, can rescue most neuromuscular and retinal axon guidance defects of *Ptp69D* mutants [Garrity et al., 1999; Sun et al., 2001]. In contrast, Newsome et al. [2000] found that a point mutation in the active site of the D1 domain of PTP69D caused defects in the guidance of R1-R6 photoreceptor axons, suggesting that the D2 domain may not be able to compensate in this genetic background. Thus, the role of catalytic activity in PTP69D signaling in vivo remains unresolved.

In a previous study, we evaluated the physiological activity of four *Ptp69D* active-site mutants [Desai and Purdy, 2003]; three of these mutant alleles affected conserved residues of the PTP loop, and one consisted of a small deletion in the WPD loop, which functions in intermediate formation and release of substrate from the catalytic site of PTPs (Fig. 1) [Zhang et al., 1994; Jia et al., 1995; Denu et al., 1996; Flint et al., 1997; Desai and Purdy, 2003]. Given the location of these mutations, each mutation could impact the catalytic activity of PTP69D. In addition, we hypothesized that the broad range of phenotypic variation in axon guidance and viability of these mutants might reflect differences in the phosphatase activity of mutant proteins. To address these questions, we transfected full-length *Ptp69D* cDNA encoding wild-type and mutant proteins into Schneider 2 (S2) cells, and assessed catalytic activity by monitoring the hydrolysis of the fluorogenic substrate DiFMUP. In the first detailed biochemical characterization of PTP69D, we show that the wild-type enzyme exhibits characteristic features of PTP-mediated hydrolysis of small molecule substrates in vitro. We find that alleles of *Ptp69D* that disrupt axon guidance have a marked effect on phosphatase activity monitored in vitro. Furthermore, we provide evidence to suggest that phosphatase-independent actions of these alleles may explain variable guidance phenotypes.

MATERIALS AND METHODS

Materials

The pRmHa3 vector and *Ptp69D* cDNA were generous gifts from Dr. Kai Zinn (California Institute of Technology). Restriction enzymes and BSA were purchased from NEB (Ipswich, MA). The QuikChange mutagenesis kit was from Stratagene (La Jolla, CA). Cell culture items including Schneider 2 (S2) cells, media, and pluronic acid, and products used to generate stable cell lines including the selection vector pCoBlast, blasticidin, and a Ca_2PO_4 transfection kit were obtained from Invitrogen (Carlsbad, CA). Other items from Invitrogen included EDTA, TEV protease for tandem affinity purification and the Colloidal Blue Stain Kit for protein quantification. Fetal bovine serum came from Atlas Biologicals (Fort Collins, CO). NP-40 was purchased from Roche Diagnostics (Indianapolis, IN). IgG Sepharose was from Amersham Biosciences (Piscataway, NJ). Amicon concentrators were obtained from Millipore (Bedford, MA). The Developmental Studies Hybridoma Bank at the University of Iowa provided 5A6, a monoclonal antibody against PTP69D. Rabbit Ig for immunoblotting was from Jackson Immunoresearch (West Grove, PA). AlexaFluor® 680 secondary antibodies were obtained from Molecular Probes, now Invitrogen. The enzymes CD45 and LAR were from Calbiochem-EMD Biosciences (San Diego, CA). PTP assay materials included 96-well Corning/Costar plates (#3631) from Krackeler Scientific, Inc. (Albany NY), FlexStation 96-well pipet tips from Molecular Devices (Sunnyvale, CA), the FlexStation monochromator from Molecular Devices (used in the Center for Molecular Neuroscience Neurochemistry Core, Vanderbilt University), and substrate 6,8-difluoro-4-methylumbelliferone (DiFMUP) and DiFMU standard from Invitrogen (Carlsbad, CA). Phosphatase inhibitors sodium orthovanadate, zinc chloride and sodium fluoride were from Sigma-Aldrich (St. Louis, MO). Magnesium chloride was purchased from Fisher Scientific (Pittsburgh, PA). PP2A holoenzyme and okadaic acid were kindly provided by Dr. Brian Wadzinski (Vanderbilt University).

Expression, Purification, and Detection of PTP69D

Primers were used to generate BglII and PacI sites in wild-type *Ptp69D* cDNA using the polymerase chain reaction (PCR). The product was then subcloned into a vector containing a tandem affinity purification (TAP) tag (pUAS-frazzled^{TAP}, courtesy of Dr. Peter Kolodziej, Vanderbilt University). Using SacI and NotI sites, TAP-tagged *Ptp69D* cDNA was subcloned

into a metallothionine-inducible S2 cell expression vector, pRmHa3. Following introduction of active site mutations using the QuikChange kit, constructs (pRmHa3-69D^{TAP}) were sequenced to verify that only the intended mutations were incorporated.

S2 cells were stably transfected with pRmHa3-69D^{TAP} constructs using a Ca_2PO_4 transfection kit and selection vector pCoBlast (Invitrogen), as described by the manufacturer. Protein expression was induced in spin flask cultures with 1 mM $CuSO_4$ at room temperature overnight. Cells were collected by centrifugation, washed with 1× PBS, and resuspended in lysis buffer (1% NP-40, 10% glycerol, 50 mM Tris HCl pH 7.5, 1 mM DTT, 5 mM EDTA, 150 mM NaCl, 0.1 mg/ml PMSF, 2 ng/ml Leupeptin, 0.02% NaN_3). Lysate was incubated overnight at 4°C and cleared at 12,000*g*. TAP-tagged protein was bound to IgG Sepharose, washed, and released with TEV protease essentially as described [Gould et al., 2004], with the following modification: lysate was incubated with IgG beads for 24–48 h, and detergent was added to buffers to a concentration between 0.1 and 1.0% NP-40. Purified protein was concentrated using Amicon concentrators, aliquotted, and stored at −80°C. Under these conditions, activity was stable for at least 2 months.

Silver staining of purified protein in 10% polyacrylamide gels was performed as described (H. Blum et al., Electrophoresis 8:93–99) or by using a Colloidal Blue Stain Kit (Invitrogen).

PTPase Assays

Continuous fluorescent reactions were generally initiated by adding 20 μL of enzyme diluted in 1× reaction buffer (50 mM MES, pH 6.0, 5 mM DTT, 2 mM EDTA, 10 μg/ml BSA), to 80 μl of 1× reaction buffer containing the appropriate substrate concentration. A 100 mM stock solution of DiFMUP in DMSO was diluted in 1× reaction buffer to give a range of final substrate concentrations from 2 to 1,500 μM DiFMUP (6,8-difluoro-4-methylumbelliferone phosphate). Except when varying specific assay conditions, reactions were performed at 25°C, pH 6.0, and the ionic strength of 0.15 M was maintained with NaCl. Reaction progress was monitored using a FlexStation monochromator (Molecular Devices), with 358 nm excitation, 455 nm emission, and 435 nm cut-off wavelengths. Arbitrary fluorescence units generated were calibrated using a DiFMU standard under assay conditions identical to those of enzyme samples.

Specific activity rates were determined by subtracting the background activity of mock-purified samples run in parallel, then adjusted to enzyme concentration. Enzyme concentrations or relative concentrations were obtained using Odyssey (LI-COR) or NIH Imaging software to quantify the density of silver-stained or colloidal coomassie-stained bands of purified enzyme relative to BSA standards. Criteria used for the collection of kinetic data included enzyme concentration in its linear range, with $[E] \ll [\text{DiFMUP}]$, a substrate concentration range of $0.25-5 \times K_m$, a substrate consumption of <5%, and a standard deviation ≤10%, except in extreme conditions, such as pH 9.0. Data were analyzed using Prism 4.0 software (GraphPad Software, Inc.). Kinetic data were generally derived from three separate experiments using a pooled preparation of purified enzyme. Variability in the kinetic properties of enzyme from assay to assay was similar in magnitude to variability between different preparations of enzyme.

pH- Response Assays

The following buffers were used to determine pH optima and pH-dependent kinetic parameters: Acetate (pH 4.0–5.5), MES (pH 5.5–6.5), Bis-Tris (pH 6.5–7.4), and TAPS (pH 7.5–9.0). Turnover rates were determined at each pH as above, taking into account the pH-sensitivity of DiFMU fluorescence. Kinetic pH-response data were fitted to the following equation:

$$k_{cat} = \frac{k_{cat}^{lim}}{1 + (H/K_1^{app}) + (K_2^{app}/H)} \qquad (1)$$

The term $k_{cat}{}^{lim}$ represents pH-independent turnover, $K_1{}^{app}$ and $K_2{}^{app}$ correspond to apparent ionization constants of the enzyme-substrate (ES) complex, and H is −log pH.

Activity of PTP69D Mutants

Sample purified from mock-transfected cells was used as a negative control for activity: a standard curve relating the concentration of this preparation to activity was used to determine background rates of DiFMUP hydrolysis. Odyssey Imaging software was used to normalize the concentration of wild-type and mutant

PTP69D ICDs. Equal amounts of enzyme were used in PTPase assays as described above.

RESULTS

Expression and Purification of PTP69D From S2 Cells

To assess the enzymatic activity of wild-type and mutant PTP69D proteins, we expressed and purified recombinant protein from S2 cells. As determined by Western blotting analysis, exogenous expression of PTP69D was relatively low, comparable to that of the endogenous protein (data not shown). Affinity purification achieved a 60-fold increase in specific activity above that of lysate, with approximately 13% recovery of PTP69D protein. The major contaminants were IgG and TEV protease, proteins involved in the purification (Fig. 2A). Purified PTP69D is stable for at least 2 months in storage at −80°C, and has a specific activity toward DiFMUP of 745 nmol/min/mg. Full-length precursor protein was detected as a band of approximately 200 kDa on an SDS polyacrylamide gel (Fig. 2A). Post-translational cleavage yielded mature extracellular and intracellular products with apparent molecular masses of 116 and 99 kDa, respectively. Besides proteolysis, further indication that exogenously expressed protein is subject to normal post-translational modifications in this cell type came from the observation that catalytically inactive PTP69D was tyrosine-phosphorylated, as observed with other RPTPs (data not shown) [Petrone and Sap, 2000; Alonso et al., 2004].

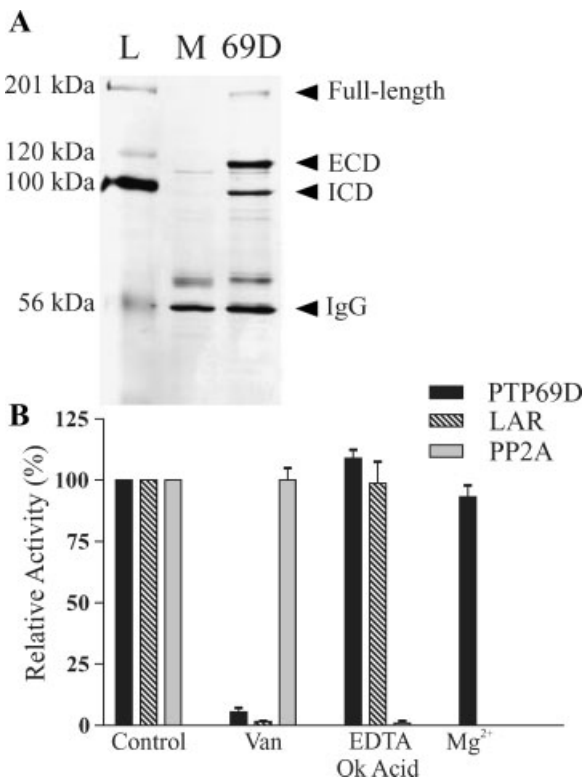

Fig. 2. Expression and specificity of PTP69D. **A**: Representative silver stain of Ig eluates from mock-transfected (M) or *Ptp69D*^{WT}-transfected (69D) cells. (L) is the molecular mass marker. Arrowheads indicate immature full-length PTP69D (~200 kDa), extracellular (~120 kDa, ECD), and intracellular (~100 kDa, ICD) domains, and IgG (~55 kDa). **B**: Activity of phosphatases PTP69D, LAR, and PP2A toward DiFMUP (1.5 mM). Control, no additions; Van, sodium orthovanadate (0.1 mM); EDTA and Ok Acid (Okadaic acid) (1 mM and 1 μM, respectively); Mg^{2+}, magnesium (1 mM). Data is expressed as mean relative activity ± SD, from three enzyme preparations.

PTP69D Activity: Specificity and Modulators

The specificity of purified PTP69D was addressed by measuring its activity toward DiFMUP in the presence of the classical tyrosine phosphatase inhibitor, vanadate, in EDTA-free buffer (Fig. 2B). A low concentration of vanadate (10 μM) inhibited a majority of PTP69D activity toward DiFMUP (Table I). Hundred-micromolar vanadate inhibited over 90% of PTP69D activity, even at substrate concentrations approximately 7.5 times greater than the K_m (1.5 mM final DiFMUP). The PTP LAR was also completely inhibited under these conditions. On the other hand, inhibitors of Ser/Thr phosphatases such as okadaic acid, EDTA,

TABLE I. Effect of Various Modulators on PTP69D Activity

Effector	Concentration	Relative activity (%)
Vanadate	10 μM	29 ± 3
	100 μM	7 ± 3
	1,000 μM	2 ± 3
$ZnCl_2$	10 μM	78 ± 2
	100 μM	48 ± 4
	1,000 μM	43 ± 5
$MgCl_2$	1 mM	96 ± 4
	10 mM	97 ± 5
	10 mM	Lysate: 85 ± 4
EDTA/NaF	1 mM/50 mM	77 ± 9
	1 mM/50 mM	Lysate: 39 ± 1
EDTA/Okadaic acid	1 mM/1 μM	109 ± 4
	1 mM/1 μM	PP2A: 1 ± 1

The standard reaction buffer consisted of 50 mM MES, pH 6.0, 150 mM NaCl, 5 mM DTT, 2 mM EDTA, and 10 μg/ml BSA. Substrate was added to a concentration equivalent to the K_m value, 180 μM. Activity is expressed as a percentage of control ± SEM that is enzyme activity in the absence of other additions. The enzyme concentration was approximately 0.1 nM. Enzyme is wild-type PTP69D except where otherwise noted. Values are the mean of single measurements from three independent assays.

and sodium fluoride, had minimal effects on PTP69D (Fig. 2B and Table I). The addition of up to 10 mM $MgCl_2$ in the absence of EDTA had no effect on the activity of PTP69D, suggesting that the preparation was not contaminated with PP2C, which is dependent upon the presence of Mg^{2+} ions for activity [Ingebritsen et al., 1983]. Mutation of the D1 domain catalytic Cys residue ($PTP69D^{D1}$) completely abolished specific activity toward DiFMUP (Fig. 6). Taken together, these data indicate that all detectable in vitro catalytic activity of PTP69D toward DiFMUP resides in the D1 domain, and that PTP69D demonstrates biochemical behavior characteristic of other tyrosine phosphatases.

PTP69D Activity: Optimal Conditions

The pH-rate profiles of phosphatases may vary depending on the substrate utilized, however, a common feature of PTPs is acidic optima for small molecule aryl phosphates. pH optima for dephosphorylation of DiFMUP by PTP69D, CD45, and LAR were determined by measuring relative rates of PTP activity in reaction buffers of graded pH and constant ionic strength. The pH optimum for PTP69D-catalyzed hydrolysis of DiFMUP was pH 6.0, slightly higher than that of CD45 and LAR, which exhibit optima at pH 5.4 and pH 5.5, respectively (Fig. 3A and data not shown). No obvious buffer-specific effects were detected, despite the fact that the buffer MES inhibits at least one tyrosine phosphatase, Yop51 [Zhang et al., 1992; Montalibet et al., 2005].

A plot of the relative activity of PTP69D versus temperature revealed that this enzyme is stable over a range of temperatures from 20 to 45°C (Fig. 3B). A higher yield of PTP69D protein was obtained when S2 cells were induced at room temperature (~22°C) as opposed to 27°C. This may signify that conditions for protein folding are improved at the lower temperature, since there was no indication of thermal denaturation below 42°C. Since *Drosophila* is a poikilothermic organism, subsequent assays were performed at 25°C to reproduce in vivo conditions.

Comparison of Kinetic Parameters of PTP69D, CD45, and LAR

The catalytic efficiency (k_{cat}/K_m) of PTP69D is comparable within one order of magnitude to values determined for CD45 and LAR using the same conditions (Table II). At approximately

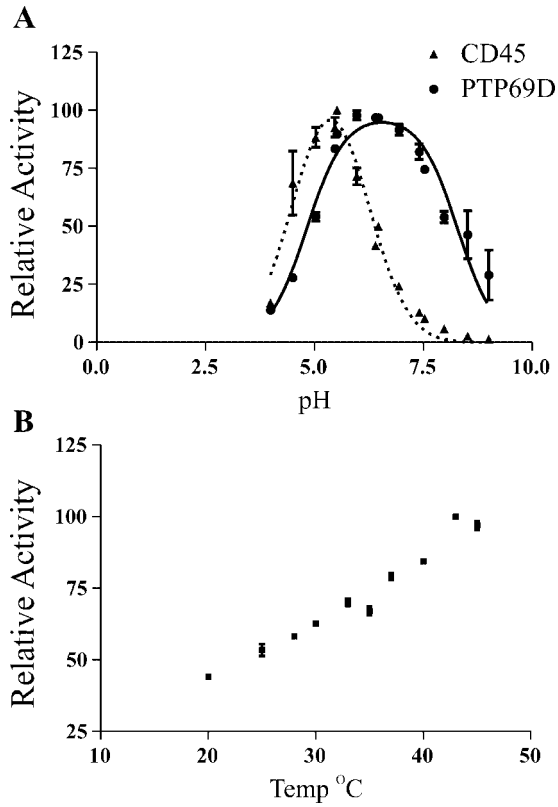

Fig. 3. Optimal conditions for PTP69D activity. **A**: pH dependence of the activity of PTP69D (● and solid line), and CD45 (▲ and dashed line) phosphatases, using DiFMUP as a substrate at concentrations of 1.2 mM and 226 μM, respectively, in buffers adjusted to various pH values (see Methods). **B**: Temperature dependence of PTP69D-mediated hydrolysis of DiFMUP (166 μM). Relative activity is expressed as % maximum, the mean ± SD, of three independent experiments.

200 μM, the K_m for PTP69D-catalyzed hydrolysis of DiFMUP is similar to published values for CD45 (156 μM), SHP2 (104 μM), and Cdc25 (420 μM) [Montalibet et al., 2005; Welte et al., 2005]. Like other tyrosine-specific

TABLE II. Kinetic Constants for the Hydrolysis of DiFMUP by PTP69D, CD45, and LAR*

	k_{cat} (/s)	K_m (μM)	k_{cat}/K_m (/M/s)
PTP69D	80	198	4.0×10^5
CD45	94	86	1.1×10^6
	214[a]	26[a]	8.2×10^{6a}
	72[b]	156[b]	4.6×10^{5b}
LAR	48	17	2.8×10^6
	19[b]	39[b]	4.9×10^{5b}

*Reaction buffer was MES pH 6.0 for PTP69D, CD45, and LAR in this study.
[a]Data published previously by Montalibet et al. [2005]. (Bis-Tris buffer, pH 6.0)
[b]Data published previously by Welte et al. [2005]. (HEPES buffer, pH 6.9)

phosphatases, and unlike the dual specificity phosphatase Cdc25 that has a k_{cat} of 0.032/s [Montalibet et al., 2005], PTP69D efficiently catalyzes hydrolysis of this substrate with a k_{cat} value of 80/s. Kinetic parameters obtained here for CD45 (k_{cat} of 94/s and K_m of 86 μM) and LAR (k_{cat} of 48/s and K_m of 17 μM) agree well with those reported previously [Montalibet et al., 2005; Welte et al., 2005].

Effect of pH on Activity of PTP69D

As opposed to a majority of PTPs, wild-type PTP69D has a Lys residue in place of the conserved hinge-region Pro in the WPD loop (Fig. 1). This substitution might alter flexibility of the loop and positioning of the conserved Asp, which acts as a general base during intermediate (E-P) hydrolysis (reviewed in: [Kolmodin and Aqvist, 2001]). Since E-P hydrolysis is the rate-limiting step of the reaction catalyzed by tyrosine-specific PTPs when small substrates are used, these differences would be reflected in the k_{cat} parameter. The typical pH-k_{cat} profile for a PTP consists of overlapping ionization curves with ascending and descending slopes of +1 and −1, respectively, reflecting the involvement of a general acid and base in E-P hydrolysis. As seen in Figure 4, the pH-k_{cat} profile of PTP69D is consistent with the conserved reaction mechanism of the PTP family, despite sequence differences in the WPD loop. The pH-independent k_{cat} value of 80 ± 2/s at approximately pH 6.5 was derived by fitting pH-response data to Eq. (1) (see Methods). Apparent ionization constants were also derived: pK_1^{app} (4.8 ± 0.1) designates the pKa of a group that must be deprotonated in PTP69D for catalysis to occur, and pK_2^{app} (8.2 ± 0.1) represents a group that must be protonated for catalysis to occur (e.g., a general acid).

Effect of Temperature on Activity of PTP69D

The Arrhenius plot of PTP69D activity versus temperature was linear and continuous between the temperatures of 20° and 45°C (Fig. 5). The lack of discontinuity indicates that there was no change in the rate-limiting step of catalysis over this temperature range. Linearity reflects the absence of significant denaturation of PTP69D protein at these temperatures within the time-course of the experiment. The slope of the line yielded an energy of activation, E_{act}, of 33.2 ± 1.3 kJ/mol which is similar to corresponding values reported for other PTPs such as PTP1B (18.4 ± 3.0 kJ/mol) and TCPTP (25.3 ± 1.2 kJ/mol) [Romsicki et al., 2003].

Effect of Active Site Mutations on PTP69D Activity

The allelic series of *Ptp69D* mutants we isolated in a previous genetic screen displays striking diversity with respect to viability and axon guidance phenotypes [Desai and Purdy, 2003]. $Ptp69D^{1}/Df(3L)^{8ex34}$ is a combination of deletion alleles that represents complete loss of PTP69D function; only 8% of mutants of this

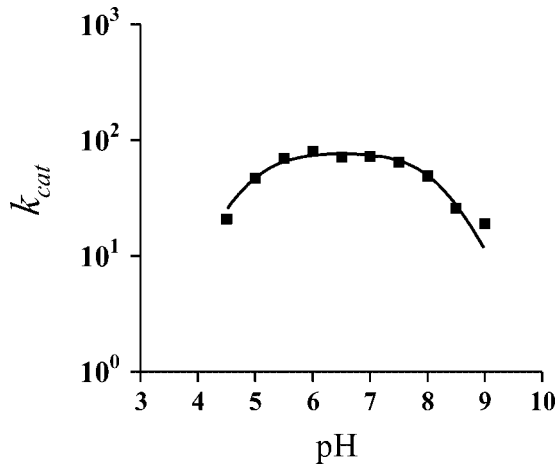

Fig. 4. Effects of pH on PTP69D-catalyzed hydrolysis of DiFMUP. Kinetic parameters were determined using assay buffers of varying pH, and data were fitted to Eq. (1) (see Methods). Data points indicate the mean ± SD from three independent experiments. Error bars, where not visible, are within the data symbols.

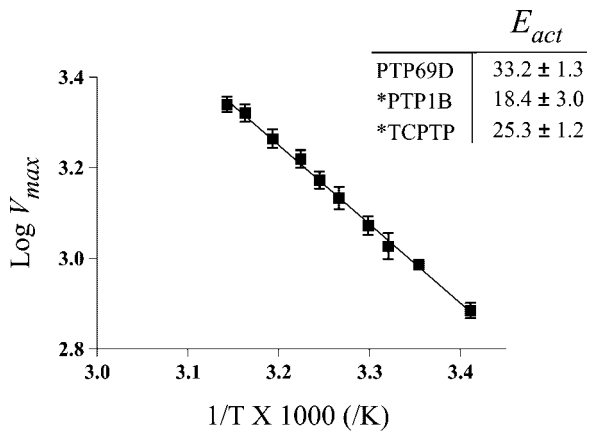

Fig. 5. Arrhenius plot of PTP69D activity versus temperature. Log V_{max} versus temperature (/K) is plotted (mean ± SD from three independent experiments). The solid line indicates the best-fit line derived from linear regression analysis. Energy of activation (inset) was calculated from the slope of this plot. * Values for PTP1B and TCPTP, previously published, are listed for comparison [Romsicki et al., 2003].

genotype survive to the pupal stage, and 26% of their ISNb motor nerves show guidance errors. Phenotypically, *Ptp69D*^{20} is a hypomorphic allele with a Ser substitution for the second invariant Gly in the 'GxGxxG' motif in the PTP-loop (Fig. 1). This mutant is almost 100% viable, and has very low penetrance defects in guidance of the ISNb motor nerve; only 8% were severe. In contrast, *Ptp69D*^{7}, which has a three amino acid deletion removing the conserved Asp of the WPD loop along with the two consecutive residues, is completely lethal prior to pupation, and has highly penetrant axon guidance defects (Fig. 1). In this case, 57% of ISNb motor nerves are affected, with 44% showing severe defects including bypass of target muscles, aberrant pathfinding within the target muscle field, and other abnormalities. On the other hand, *Ptp69D*^{21}, which has a Tyr in place of the catalytic Cys, has an intermediate phenotype with about 11% of larvae surviving to the pupal stage, and 32% total defects in ISNb guidance [Desai and Purdy, 2003]. Although *Ptp69D*^{Y125} has not been characterized with respect to motor axon guidance, this mutant manifests lethality and retinal axon guidance defects similar in penetrance to *Ptp69D*^{Y100} and *Ptp69D*^{Y98}, truncation alleles with early nonsense mutations, [Newsome et al., 2000; Desai and Purdy, 2003] (Fig. 1). Interestingly, mutant alleles bearing the same mutations as *Ptp69D*^{21} and *Ptp69D*^{Y125} were recovered in the closely related *C. elegans* RPTP, *Clr-1* (alleles *gm30* and *n1660*, respectively). Both *Clr-1* alleles are classified as strong loss of function alleles according to phenotypic criteria, though the biochemical activity of these mutant proteins is unknown [Kokel et al., 1998]. Whereas *Ptp69D*^{Y125} showed somewhat reduced protein staining by immunohistochemistry, *Ptp69D*^{20}, *Ptp69D*^{21}, and *Ptp69D*^{7} all expressed wild-type levels of protein, suggesting that some other biochemical property of these proteins explains these differing phenotypes [Desai and Purdy, 2003].

To test the biochemical function of mutant proteins and to determine whether differences in catalytic activity could account for their varying phenotypes, we expressed wild-type and mutant *Ptp69D* cDNA in S2 cells. Equal amounts of mutant ICDs were tested for enzymatic activity in an in vitro reaction with DiFMUP as a substrate, and rates of turnover were normalized to that of an equivalent amount of wild-type ICD (Fig. 6A). Mutants with inactivating Cys to Ser substitutions in the "catalytic" residue of one or both PTP domains (PTP69D^{D1} and PTP69D^{D1D2}) were included as negative controls. Turnover of DiFMUP was reduced to near-background levels for every mutant, even when the concentration of mutant ICD was 15 times that of the wild-type protein (Fig. 6B). Rates of DiFMUP hydrolysis were less than 0.6% that of wild-type PTP69D for all mutants. The difference in activity between wild-type enzyme and all mutants was statistically significant ($P < 0.001$), whereas the difference in activity between mutants was not ($P > 0.05$). Due to low activity of the mutants, even at high substrate concentrations, we were unable to determine kinetic parameters for turnover of DiFMUP.

Since the in vivo phenotypes of *Ptp69D*^{20} are temperature-sensitive [Desai and Purdy, 2003], with greater viability and lower axon guidance

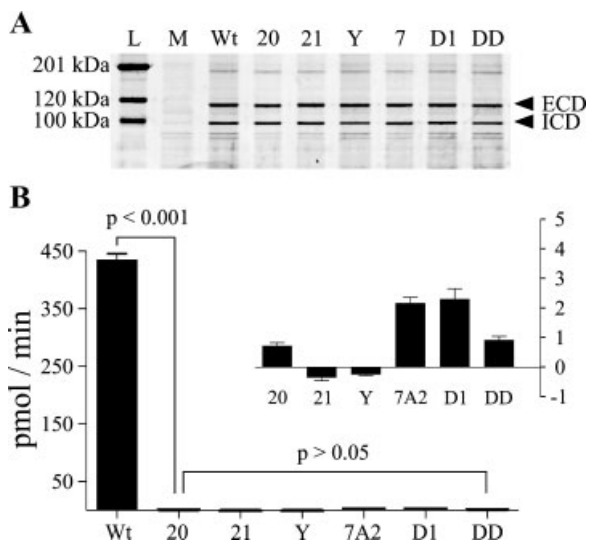

Fig. 6. Biochemical activity of PTP69D mutant proteins. **A**: Representative gel showing equal loading of wild-type and mutant PTP69D ICD, visualized with colloidal coomassie. L, molecular mass marker; M, mock-transfected; Wt, wild-type PTP69D; 20, PTP69D^{20}; 21, PTP69D^{21}; Y, PTP69D^{Y125}; 7, PTP69D^{7}; D1, PTP69D^{D1}; DD, PTP69D^{D1D2}; ECD, extracellular domain; ICD, intracellular domain. **B**: Rates of DiFMUP hydrolysis expressed as mean ± SD of three independent experiments. In this assay, enzyme concentrations were approximately 0.15 nM for wild-type PTP69D and 2.2 nM for mutants—rates were normalized accordingly. A substrate concentration of 1.5 mM DiFMUP was used. Mutant activity rates were never more than twofold above background, and rates for PTP69D^{21} and PTP69D^{Y125} were not reliably above background (see inset). Inset: mutant data plotted on an expanded y axis. Data were analyzed using one-way ANOVA followed by a Bonferroni post-test.

defects exhibited at the permissive temperature (18°C), we explored the possibility that activity of the enzyme might be higher at reduced temperature. While we found that inducing protein expression at 18°C increased enzyme activity about two-fold, the temperature of the enzyme assay had little effect on the activity of PTP69D^{20}. The activity of PTP69D^{20} was never raised relative to the control D1-inactive mutant, suggesting that temperature-sensitivity may be related to differences in protein folding (data not shown). Taken together, these data indicate that mutations that eliminate the activity of PTP69D have an impact on its function in axon guidance and viability; however, the phenotypic variability of *Ptp69D* mutants is unrelated to the in vitro efficiency of the enzyme.

DISCUSSION

We have demonstrated for the first time that *Drosophila* PTP69D is a tyrosine phosphatase with a catalytic efficiency comparable to that of other tyrosine-specific phosphatases. This is notable because the sequence of the catalytically important WPD loop is divergent in PTP69D. In place of the first Pro, conserved in over 90% of PTPs [Andersen et al., 2001], PTP69D has a Lys residue (see Fig. 1 for conserved motif). Interestingly, in a recent study investigating the role of various amino acids in the WPD loop of SHP-1, the authors did not mutate the first conserved Pro because they assumed that it would disrupt the activity of the enzyme [Yang et al., 2001]. Even the *Yersinia* PTP, which has a WPD loop that diverges significantly in sequence from other organisms, retains the first conserved Pro (WPDQTAV). Nevertheless, the response of PTP69D to modulators of activity, its catalytic efficiency, and its pH-k_{cat} profile all suggest that PTP69D shares a common tyrosine phosphatase reaction mechanism, likely conserving the role of the Asp of the WPD loop in intermediate formation and hydrolysis. In short, our biochemical characterization shows that the kinetic properties of PTP69D are consistent with those of other PTPs.

A number of studies evaluate the effects of chemical or site-directed mutagenesis on the activity of PTPs [Streuli et al., 1990; Andersen et al., 2001]. Amino acids in the active site of PTPs are variably sensitive to substitution; some mutations eliminate catalytic activity completely, while others retain up to 10–25% of wild-type activity in vitro [Streuli et al., 1990; Johnson et al., 1992]. The impact of these mutations on the in vivo function of the PTP is difficult to address, however. The advantage of using EMS-induced alleles of *Ptp69D* as tools is that one can directly test the assumption that the enzymatic activity of PTP69D is required for its functions in viability and axon guidance.

Based on previous in vitro work, the effect of mutating the catalytic Cys1097 is predictable; we expected this mutation to completely eliminate the tyrosine phosphatase activity of PTP69D^{21}, as is invariably seen with PTPs [Guan and Dixon, 1991; Barford et al., 1998]. Mutations in the WPD loop, as seen with PTP69D^{7} (Fig. 1) were also expected to decrease activity significantly, since the conserved Asp implicated in both intermediate formation and hydrolysis is missing. Even a conservative mutation of Asp to Asn in the WPD loop of the dual specificity phosphatase VHR resulted in a 100-fold decrease in activity, and the same substitution resulted in a decrease of similar magnitude in the k_{cat} of tyrosine-specific PTP1B [Denu et al., 1995; Lohse et al., 1997]. Predicting the catalytic consequences of Gly1102Ser and Gly1105Arg mutations is less obvious. No specific function has been described for the second Gly (1102) in the GxGxxG motif except for hydrophobic interaction with the pTyr of the substrate. However, this interaction involves main-chain amide groups in this amino acid, not the side chain [Andersen et al., 2001]. Mutation of the equivalent residue to an Ala in CD45 results in a fivefold reduction of activity toward a peptide substrate, suggesting that substitution with a bulkier amino acid might have subtle effects on the structure or conformational flexibility of the PTP-loop [Johnson et al., 1992]. These results suggested that this position is somewhat tolerant to substitution, and therefore PTP69D^{20} might have residual activity. The third Gly in the GXGXXG motif, mutated in PTP69D^{Y125}, may be more sensitive to substitution, as mutation of this residue to an Ala has been shown to decrease the catalytic activity of CD45 10-fold [Johnson et al., 1992]. Since this residue is also part of a predicted helical secondary structure, it is possible that the nonconservative substitution of Arg may destabilize the PTP-loop. Thus, it seemed likely that

$PTP69D^{Y125}$, if it retained any catalytic activity at all, would be less active than $PTP69D^{20}$.

Based upon the severity of axon guidance defects and lethality, one might have predicted the rank order of phosphatase activity to be $PTP69D^{WT} > PTP69D^{20} > PTP69D^{Y125} \approx PTP69D^{21} > PTP69D^{7}$. Our finding that PTP69D mutants were equally inactive toward the substrate DiFMUP suggests that catalytic activity does not contribute to the phenotypic variation displayed by these mutants. It would appear, then, that a phosphatase-independent action of PTP69D is required for its in vivo roles in promoting normal viability and axon guidance. This conclusion is supported by the fact that *Ptp69D*^{20}, which is unable to hydrolyze DiFMUP at a rate significantly above background, is almost completely viable, and has few axon guidance defects [Desai and Purdy, 2003]. It also explains the observation that a transgene rescue construct bearing a D1-inactivating point mutation is able to rescue retinal axon guidance defects of *Ptp69D* mutants [Garrity et al., 1999].

A model of PTP69D signaling in which the active site functions as an adapter or phosphotyrosine-binding domain could be evoked to account for phenotypic differences in these mutants. Active site mutations would disrupt signaling or localization of PTP69D by affecting its ability to bind tyrosine-phosphorylated effectors or scaffolding proteins. Thus, the higher phenotypic severity of *Ptp69D*^{21} relative to *Ptp69D*^{20} may be due to the addition of a bulky tyrosyl group to the active site, a perturbation that might be anticipated to alter binding of target proteins. If the introduction of an Arg to the helix adjacent to the active site either eliminates target binding or destabilizes $PTP69D^{Y125}$ protein, this may explain why this mutant approximates the null phenotype in Newsome's study [Newsome et al., 2000]. On the other hand, the high penetrance defects of *Ptp69D*^{7} could be attributed to enhanced binding of this mutant to downstream targets. Mutation of the catalytically important Asp in the WPD loop results in an enzyme that can stably associate with its substrate without efficient hydrolysis [Flint et al., 1997]. Therefore, $PTP69D^{7}$ may act as a 'substrate-trap,' competing with other RPTPs for shared effectors. This is supported by the fact that the phenotype of *Ptp69D*^{7} resembles that of a double mutant of *Ptp69D* and *Dlar* in severity, and implies that the ability of PTP69D protein to interact with downstream targets with appropriate kinetics is critical for its in vivo function [Desai and Purdy, 2003]. Another possibility is that shortening of the WPD loop in $PTP69D^{7}$ exposes the active site, leading to indiscriminate interactions with downstream targets of other RPTPs. However, because we cannot determine kinetic parameters for hydrolysis of DiFMUP by $PTP69D^{7}$ we are unable to test these hypotheses directly.

Although we endeavored to mimic in vivo conditions in our enzyme assays, we cannot exclude the possibility that our results do not accurately reflect the in vivo biochemical activity of the mutants. Important modifications of PTP69D protein may not occur in S2 cells. For example, if alternative splicing is necessary to produce the biologically relevant form of PTP69D, our expression of the full-length cDNA construct would be problematic [Charbonneau and Tonks, 1992; Alonso et al., 2004]. In addition, conditions ideal for purifying wild-type enzyme and measuring its activity may be suboptimal for use with the mutant enzyme. Alternatively, our in vitro assays might lack an essential cofactor that would enhance activity of the mutants relative to wild-type. Finally, our choice of substrate might mask the activity of the mutants. Since amino acids external to the active site may support binding of legitimate substrates, the use of the small molecule substrate DiFMUP could exaggerate the differences in activity between wild-type and mutant PTP69D. Indeed, one previous study showed that a PTP mutant inactive toward the small molecule substrate pNPP had only slightly less activity than wild-type enzyme when the protein substrate RCML was used [Muise et al., 1996]. Since studies are currently limited to the use of artificial substrates, the hypothesis that catalytic activity is required for the function of PTP69D should be retested when in vivo targets are identified.

Our study predicts that some property of PTP69D mutant proteins other than catalytic activity, possibly related to binding of target proteins, may explain their biological diversity and be utilized in the future to verify the identity of downstream targets. These mutants may also be useful in further structure-function studies, and/or to dissect different PTP69D-mediated signaling pathways. For example, Garrity et al. [1999] find that a D2-inactive

transgene construct can rescue retinal axon guidance defects, but cannot rescue viability of *Ptp69D* mutants. Since D1-inactivating mutations affect retinal guidance [Newsome et al., 2000], this suggests that the function of the D2 domain is partially dependent upon the D1 domain, and might explain why no one has recovered a D2 domain mutation in genetic screens for loss of PTP69D function. Thus, a mutant like $Ptp69D^{20}$ could be used to screen for second-site mutations that decrease viability, in order to uncover the role of the D2 domain in vivo. The fact that delivering PTP69D protein to neurons can restore viability of *Ptp69D* mutants suggests that its function in promoting normal axon guidance is linked to its requirement for viability. However, it remains possible that these functions reflect divergent signaling pathways in neurons. Mutants like $Ptp69D^{20}$ and $Ptp69D^{10}$, which are almost completely viable but have axon guidance phenotypes of differing severity, could be used to distinguish between these pathways [Desai and Purdy, 2003]. It is clear that elucidation of the function of PTP69D and other receptor tyrosine phosphatases awaits identification of legitimate in vivo ligands and binding partners. Combining biochemical and genetic methodology, Fox and Zinn [2005] performed a deficiency screen together with immunohistochemical analysis to identify a heparan sulfate proteoglycan as an in vivo ligand for RPTP family member DLAR [Fox and Zinn, 2005]. Although ligands of this class may not bind PTP69D, since it lacks heparin-binding motifs, the approach taken to identify this ligand is feasible for PTP69D. When ligands and downstream targets of PTP69D are identified, a model for signaling can be tested by examining the effects of ligand binding on interaction with downstream targets.

ACKNOWLEDGMENTS

We thank members of the Vanderbilt community for helpful discussions in preparation of this manuscript. We are grateful to the Molecular Recognition core facility (Vanderbilt University), funded by awards CA68485 and EB00672 from the National Institutes of Health, for use of supplies and equipment. We also thank the Center for Molecular Neuroscience Neurochemistry Core (Vanderbilt University) for use of the FlexStation monochromator (Molecular Devices). J.E.P. was supported by a Training Program in Developmental Biology grant from the NIH (5T32-HD0750205). This work was also supported by awards to C.J.D. from the NIH (NSHD-38141) and the March of Dimes Birth Defects Foundation (Basil O'Conner Starter Scholars Award, 5-FY99-0111).

REFERENCES

Alonso A, Sasin J, Bottini N, Friedberg I, Osterman A, Godzik A, Hunter T, Dixon J, Mustelin T. 2004. Protein tyrosine phosphatases in the human genome. Cell 117: 699–711.

Andersen JN, Mortensen OH, Peters GH, Drake PG, Iversen LF, Olsen OH, Jansen PG, Andersen HS, Tonks NK, Moller NP. 2001. Structural and evolutionary relationships among protein tyrosine phosphatase domains. Mol Cell Biol 21:7117–7136.

Barford D, Das AK, Egloff MP. 1998. The structure and mechanism of protein phosphatases: Insights into catalysis and regulation. Annu Rev Biophys Biomol Struct 27: 133–164.

Charbonneau H, Tonks NK. 1992. 1002 protein phosphatases? Annu Rev Cell Biol 8:463–493.

Denu JM, Zhou G, Guo Y, Dixon JE. 1995. The catalytic role of aspartic acid-92 in a human dual-specific protein-tyrosine-phosphatase. Biochemistry 34:3396–3403.

Denu JM, Lohse DL, Vijayalakshmi J, Saper MA, Dixon JE. 1996. Visualization of intermediate and transition-state structures in protein-tyrosine phosphatase catalysis. Proc Natl Acad Sci USA 93:2493–2498.

Desai C, Purdy J. 2003. The neural receptor protein tyrosine phosphatase DPTP69D is required during periods of axon outgrowth in *Drosophila*. Genetics 164:575–588.

Desai CJ, Gindhart JG, Jr., Goldstein LS, Zinn K. 1996. Receptor tyrosine phosphatases are required for motor axon guidance in the *Drosophila* embryo. Cell 84:599–609.

Desai CJ, Krueger NX, Saito H, Zinn K. 1997a. Competition and cooperation among receptor tyrosine phosphatases control motoneuron growth cone guidance in *Drosophila*. Development 124:1941–1952.

Desai CJ, Sun Q, Zinn K. 1997b. Tyrosine phosphorylation and axon guidance: Of mice and flies. Curr Opin Neurobiol 7:70–74.

Ensslen-Craig SE, Brady-Kalnay SM. 2004. Receptor protein tyrosine phosphatases regulate neural development and axon guidance. Dev Biol 275:12–22.

Flint AJ, Tiganis T, Barford D, Tonks NK. 1997. Development of "substrate-trapping" mutants to identify physiological substrates of protein tyrosine phosphatases. Proc Natl Acad Sci USA 94:1680–1685.

Fortin M, Steff AM, Felberg J, Ding I, Schraven B, Johnson P, Hugo P. 2002. Apoptosis mediated through CD45 is independent of its phosphatase activity and association with leukocyte phosphatase-associated phosphoprotein. J Immunol 168:6084–6089.

Fox AN, Zinn K. 2005. The heparan sulfate proteoglycan syndecan is an in vivo ligand for the *Drosophila* LAR receptor tyrosine phosphatase. Curr Biol 15:1701–1711.

Garrity PA, Lee CH, Salecker I, Robertson HC, Desai CJ, Zinn K, Zipursky SL. 1999. Retinal axon target selection in *Drosophila* is regulated by a receptor protein tyrosine phosphatase. Neuron 22:707–717.

Gould KL, Ren L, Feoktistova AS, Jennings JL, Link AJ. 2004. Tandem affinity purification and identification of protein complex components. Methods 33:239–244.

Guan KL, Dixon JE. 1991. Evidence for protein-tyrosine-phosphatase catalysis proceeding via a cysteine-phosphate intermediate. J Biol Chem 266:17026–17030.

Ingebritsen TS, Stewart AA, Cohen P. 1983. The protein phosphatases involved in cellular regulation. 6. Measurement of type-1 and type-2 protein phosphatases in extracts of mammalian tissues; an assessment of their physiological roles. Eur J Biochem 132:297–307.

Jia Z, Barford D, Flint AJ, Tonks NK. 1995. Structural basis for phosphotyrosine peptide recognition by protein tyrosine phosphatase 1B. Science 268:1754–1758.

Jiang G, den Hertog J, Su J, Noel J, Sap J, Hunter T. 1999. Dimerization inhibits the activity of receptor-like protein-tyrosine phosphatase-alpha. Nature 401:606–610.

Johnson KG, Van Vactor D. 2003. Receptor protein tyrosine phosphatases in nervous system development. Physiol Rev 83:1–24.

Johnson P, Ostergaard HL, Wasden C, Trowbridge IS. 1992. Mutational analysis of CD45. A leukocyte-specific protein tyrosine phosphatase. J Biol Chem 267:8035–8041.

Kokel M, Borland CZ, DeLong L, Horvitz HR, Stern MJ. 1998. *clr-1* encodes a receptor tyrosine phosphatase that negatively regulates an FGF receptor signaling pathway in *Caenorhabditis elegans*. Genes Dev 12:1425–1437.

Kolmodin K, Aqvist J. 2001. The catalytic mechanism of protein tyrosine phosphatases revisited. FEBS Lett 498: 208–213.

Krueger NX, Reddy RS, Johnson K, Bateman J, Kaufmann N, Scalice D, Van Vactor D, Saito H. 2003. Functions of the ectodomain and cytoplasmic tyrosine phosphatase domains of receptor protein tyrosine phosphatase Dlar in vivo. Mol Cell Biol 23:6909–6921.

Lohse DL, Denu JM, Santoro N, Dixon JE. 1997. Roles of aspartic acid-181 and serine-222 in intermediate formation and hydrolysis of the mammalian protein-tyrosine-phosphatase PTP1. Biochemistry 36:4568–4575.

Maurel-Zaffran C, Suzuki T, Gahmon G, Treisman JE, Dickson BJ. 2001. Cell-autonomous and -nonautonomous functions of LAR in R7 photoreceptor axon targeting. Neuron 32:225–235.

Montalibet J, Skorey KI, Kennedy BP. 2005. Protein tyrosine phosphatase: Enzymatic assays. Methods 35: 2–8.

Muise ES, Vrielink A, Ennis MA, Lemieux NH, Tremblay ML. 1996. Thermosensitive mutants of the MPTP and hPTP1B protein tyrosine phosphatases: Isolation and structural analysis. Protein Sci 5:604–613.

Newsome TP, Asling B, Dickson BJ. 2000. Analysis of *Drosophila* photoreceptor axon guidance in eye-specific mosaics. Development 127:851–860.

Petrone A, Sap J. 2000. Emerging issues in receptor protein tyrosine phosphatase function: Lifting fog or simply shifting? J Cell Sci 113(Pt 13):2345–2354.

Romsicki Y, Kennedy BP, Asante-Appiah E. 2003. Purification and characterization of T cell protein tyrosine phosphatase reveals significant functional homology to protein tyrosine phosphatase-1B. Arch Biochem Biophys 414:40–50.

Singh DK, Kumar D, Siddiqui Z, Basu SK, Kumar V, Rao KV. 2005. The strength of receptor signaling is centrally controlled through a cooperative loop between Ca2+ and an oxidant signal. Cell 121:281–293.

Stoker AW. 2001. Receptor tyrosine phosphatases in axon growth and guidance. Curr Opin Neurobiol 11:95–102.

Streuli M, Krueger NX, Thai T, Tang M, Saito H. 1990. Distinct functional roles of the two intracellular phosphatase like domains of the receptor-linked protein tyrosine phosphatases LCA and LAR. Embo J 9:2399–2407.

Sun Q, Bahri S, Schmid A, Chia W, Zinn K. 2000a. Receptor tyrosine phosphatases regulate axon guidance across the midline of the *Drosophila* embryo. Development 127:801–812.

Sun QL, Wang J, Bookman RJ, Bixby JL. 2000b. Growth cone steering by receptor tyrosine phosphatase delta defines a distinct class of guidance cue. Mol Cell Neurosci 16:686–695.

Sun Q, Schindelholz B, Knirr M, Schmid A, Zinn K. 2001. Complex genetic interactions among four receptor tyrosine phosphatases regulate axon guidance in *Drosophila*. Mol Cell Neurosci 17:274–291.

Tonks NK. 2005. Redox redux: Revisiting PTPs and the control of cell signaling. Cell 121:667–670.

Welte S, Baringhaus KH, Schmider W, Muller G, Petry S, Tennagels N. 2005. 6,8-Difluoro-4-methylumbiliferyl phosphate: A fluorogenic substrate for protein tyrosine phosphatases. Anal Biochem 338:32–38.

Yang J, Niu T, Zhang A, Mishra AK, Zhao ZJ, Zhou GW. 2001. Relation between the flexibility of the WPD loop and the activity of the catalytic domain of protein tyrosine phosphatase SHP-1. J Cell Biochem 84:47–55.

Zhang ZY, Clemens JC, Schubert HL, Stuckey JA, Fischer MW, Hume DM, Saper MA, Dixon JE. 1992. Expression, purification, and physicochemical characterization of a recombinant *Yersinia* protein tyrosine phosphatase. J Biol Chem 267:23759–23766.

Zhang ZY, Wang Y, Dixon JE. 1994. Dissecting the catalytic mechanism of protein-tyrosine phosphatases. Proc Natl Acad Sci USA 91:1624–1627.